

# We are IntechOpen, the world's leading publisher of Open Access books Built by scientists, for scientists

4,600

Open access books available

119,000

International authors and editors

135M

Downloads

Our authors are among the

154

Countries delivered to

TOP 1%

most cited scientists

12.2%

Contributors from top 500 universities



WEB OF SCIENCE™

Selection of our books indexed in the Book Citation Index  
in Web of Science™ Core Collection (BKCI)

Interested in publishing with us?  
Contact [book.department@intechopen.com](mailto:book.department@intechopen.com)

Numbers displayed above are based on latest data collected.  
For more information visit [www.intechopen.com](http://www.intechopen.com)



# Role of Optical Coherence Tomography in the Evaluation and Management of Glaucoma

*Baswati Sahoo and Julie Pegu*

## Abstract

Glaucoma is the leading cause of irreversible, yet preventable, blindness throughout the world. Since it is a disease which can be treated but not cured, it is crucial for the treating ophthalmologist to catch the disease as early as possible. The diagnosis of glaucoma is currently based on the appearance of the optic disc and standard achromatic perimetry. However, to detect glaucoma in its early stages, there are various diagnostic modalities of which optical coherence tomography serves as a novel tool. Optical coherence tomography has emerged over the years with the ability to detect changes in the optic nerve head, retinal nerve fiber layer, and currently the ganglion cell layer much earlier than the defects manifest functionally. Thus, optical coherence tomography acts as an important diagnostic aid to diagnose and monitor the progression of this sight threatening disease called glaucoma.

**Keywords:** optical coherence tomography, pre perimetric glaucoma, ganglion cell complex, retinal nerve fiber layer, spectral domain optical coherence tomography, time domain optical coherence tomography

## 1. Introduction

From the early days until the turn of the twentieth century, glaucoma was defined as “pressure within the eye higher than the statistical normal of the population.” It was thought that this rise in pressure caused damage to the optic nerve that was irreversible. It is not until the end of twentieth century, when newer concepts such as the ocular hypertension and the normal tension glaucoma emerged, which led people to challenge this definition [1]. Glaucoma then was redefined by the American Academy of Ophthalmology as an optic neuropathy with characteristic structural damage to optic nerve, associated with progressive retinal ganglion cell death, loss of nerve fibers, and visual field loss. However, the intraocular pressure was considered as the strongest risk factor and possibly the only modifiable one [2].

## 2. Why optic nerve?

Optic nerve evaluation is the cornerstone of management of glaucoma. It remains the most crucial step in the early diagnosis of glaucoma and monitoring progressive nerve damage. Stereoscopic changes in the optic nerve head and retinal nerve fiber layer, which are seen clinically, are actually the manifestations of loss

of the ganglion cell layer which cannot be seen using slit lamp biomicroscopy. Moreover, since the structural abnormalities precede the functional changes, it is imperative to have an objective, quantitative, and reproducible imaging technique which is capable of early diagnosis and helps monitoring of the disease.

There are various imaging modalities being used by glaucoma experts today. Confocal scanning laser ophthalmoscopy (HRT; Heidelberg Retina Tomography; Heidelberg Engineering, Heidelberg, Germany), scanning laser polarimetry (GDx; Carl Zeiss Meditec, Dublin, California, USA), and optical coherence tomography (OCT; Carl Zeiss Meditec and others) are among the popular ones. However, subjective optic disc evaluation with stereo optic disc photography still remains the mainstay of every clinical practice.

### **3. Concept of preperimetric glaucoma**

Glaucomatous optic neuropathy is characterized by structural changes in the optic disc in the form of thinning of neuroretinal rim, pallor, and progressive cupping of the optic disc. Since it is a disease which can be treated but not cured, it is crucial for the treating ophthalmologist to catch the disease in its early stages. In glaucoma, structural injury has been documented to precede functional injury in most eyes [3]. One of the reasons observed by many researchers was that it took almost a loss of 40% of the ganglion cells to pick up a defect on the standard automated perimetry. Recently, a change in the diagnostic criteria of glaucoma has been promoted so that glaucoma diagnosis may be made before the old prerequisites functional criteria of standard automatic perimetry visual field (SAP-VF) loss are apparent, namely the “preperimetric glaucoma” (PPG).

To be diagnosed as a case of PPG, a patient needs to have a structural injury to the optic nerve head (ONH) sufficient enough to be classified under glaucomatous optic neuropathy (GON) and ought to be clinically proven. The introduction of newer imaging devices such as confocal scanning laser ophthalmoscopy, scanning laser polarimetry, and optical coherence tomography for measuring structural changes in the optic nerve head and retinal nerve fiber layer seems promising for early detection of glaucoma. Although an effort has been made to diagnose glaucoma in its early stages, there is no evidence that a single measurement is superior to the others and a combination of tests may be needed for detecting early damage in glaucoma.

### **4. Diagnostic aids in preperimetric glaucoma**

Standard automated perimetry is the gold standard in the diagnosis of glaucoma as it gives us an assessment of the functional loss occurring in glaucoma. Optic disc photography gives a structural assessment of the optic nerve and surrounding nerve fiber layer but can be challenging due to inter-individual variability. Serial 3D imaging on the other hand may seem to be a better way of the subjective diagnosis of glaucomatous optic neuropathy during its early stages [4, 5]. Capturing early loss of retinal nerve fibers both clinically and by means of red-free photos may not be easy and sometimes could be indecisive, particularly in diffuse than in localized retinal nerve fibers loss [6].

### **5. Optical coherence tomography (OCT)**

Optical coherence tomography (OCT) is a non-invasive diagnostic technique that renders an *in vivo* cross-sectional view of the retina, retinal nerve fiber layer, and the

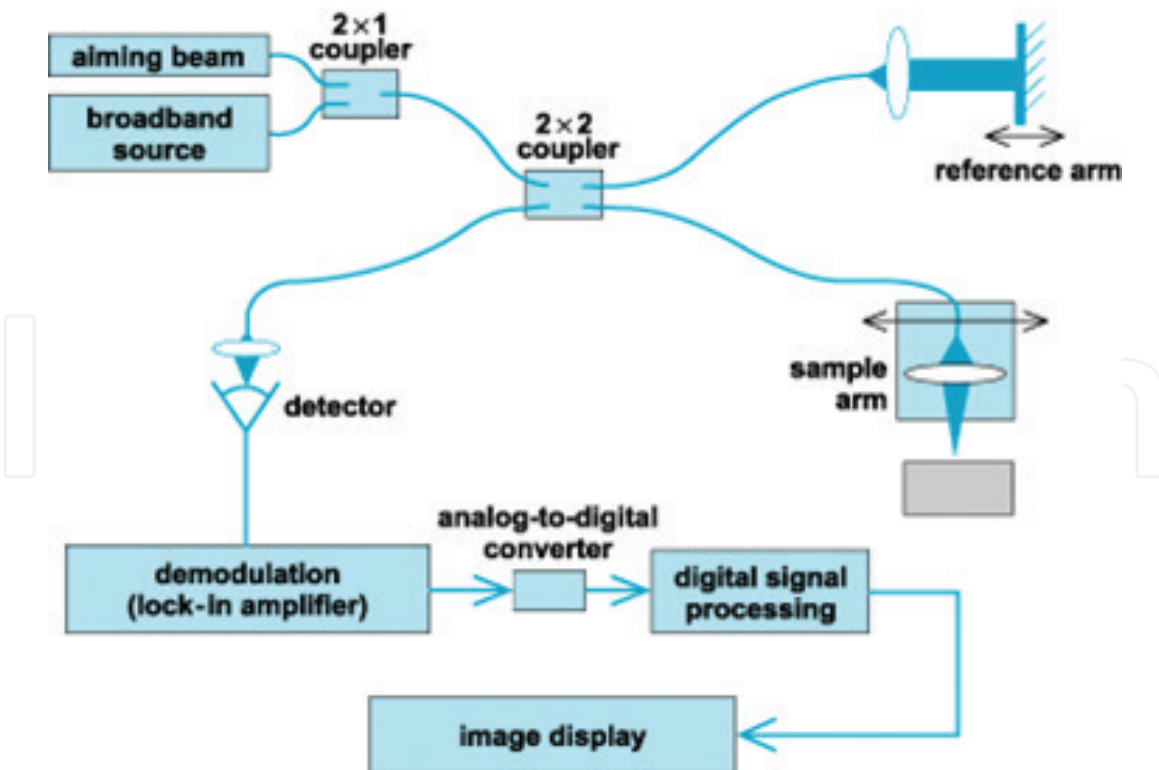


**Figure 1.**  
 Principle of optical coherence tomography.

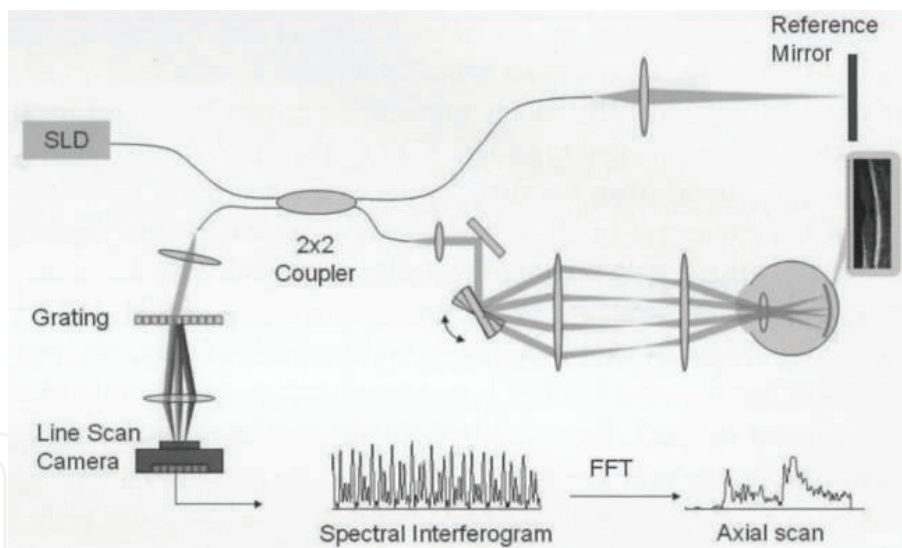


**Figure 2.**  
 Principle of Fourier domain optical coherence tomography.

optic nerve head. OCT utilizes a concept known as low coherence interferometry. A broadband width light from a superluminescent diode is projected onto the retina. This is divided into a reference and a sample beam, and further the echo time delays of light reflected from the retina as well as reference mirror at known distances is compared. The light waves that are backscattered from the retina, interfere with the reference beam, and this interference pattern is measured by a photodetector (**Figure 1**). This is the basic principle on which the Satus OCT works.

Spectral domain OCT (SD-OCT) also works on similar principles, however, with a much higher data acquisition speed as compared to TD-OCT. This is achieved by the Michelson type interferometer with a stationary reference mirror. Instead of the interference signal being captured by a point detector, after the two returning beams

recombine and form the interference pattern at the beam splitter, the interference pattern is split by a grating into its frequency components, all of these components are simultaneously detected by a charge-coupled device (CCD) (**Figure 2**). SD-OCT is also known as Fourier domain OCT (FD-OCT) because the distances are encoded in the Fourier transform of the frequencies of light reflected.

## **6. Spectrum of OCT in the diagnosis of glaucoma**

The OCT can scan the optic nerve head (ONH), peripapillary retinal nerve fiber (RNFL), and the macular area (GCC—ganglion cell complex). An addition to the spectrum of posterior evaluation is the anterior segment OCT (AS-OCT) which utilizes a higher wavelength light to capture images of the anterior chamber angle.

## **7. Types of OCT**

### **7.1 Stratus or time domain OCT**

From its inception, OCT images were acquired in a time domain fashion. Time domain systems acquire approximately 400 A-scans per second using 6 radial slices oriented 30° apart. Time-domain OCT (TD-OCT) systems featured scan rates of 400 A-scans per second with an axial resolution of 8–10 μm in tissue [7]. Since the slices are 30° apart, there always is a possibility to miss pathology between the slices.

### **7.2 Fourier domain OCT (FD-OCT) or spectral domain OCT (SD-OCT)**

SD-OCT, on the other hand, achieves scan rates of 20,000–52,000 A-scans per second and a resolution of 5–7 μm in tissue [8, 9]. This increased scan rate and number diminishes the likelihood of motion artifact, enhances the resolution, and decreases the chance of missing lesions.

### **7.3 Anterior segment OCT (AS-OCT)**

Anterior segment OCT utilizes higher wavelength light (1310 nm) as compared to 830 nm of traditional posterior segment OCT. This higher wavelength light results in greater absorption and less penetration allowing clear images of the parts of the anterior segment (cornea, anterior chamber, iris, and angle). Currently, there are two commercially produced dedicated anterior segment devices, the slit lamp-OCT (SL-OCT: Heidelberg Engineering) and the Visante (Carl Zeiss Meditec, Inc.).

## **8. Clinical interpretation of OCT in glaucoma diagnosis**

### **8.1 Stratus OCT (Carl Zeiss)**

The Stratus OCT utilizes various protocols for analysis of the optic nerve head and the retinal nerve fiber layer.

#### *8.1.1 Optic nerve head analysis*

The “Fast Optic disc “ pattern is used to analyze the optic nerve head. It consists of six evenly placed radial lines centered on the optic nerve head. Each of the six

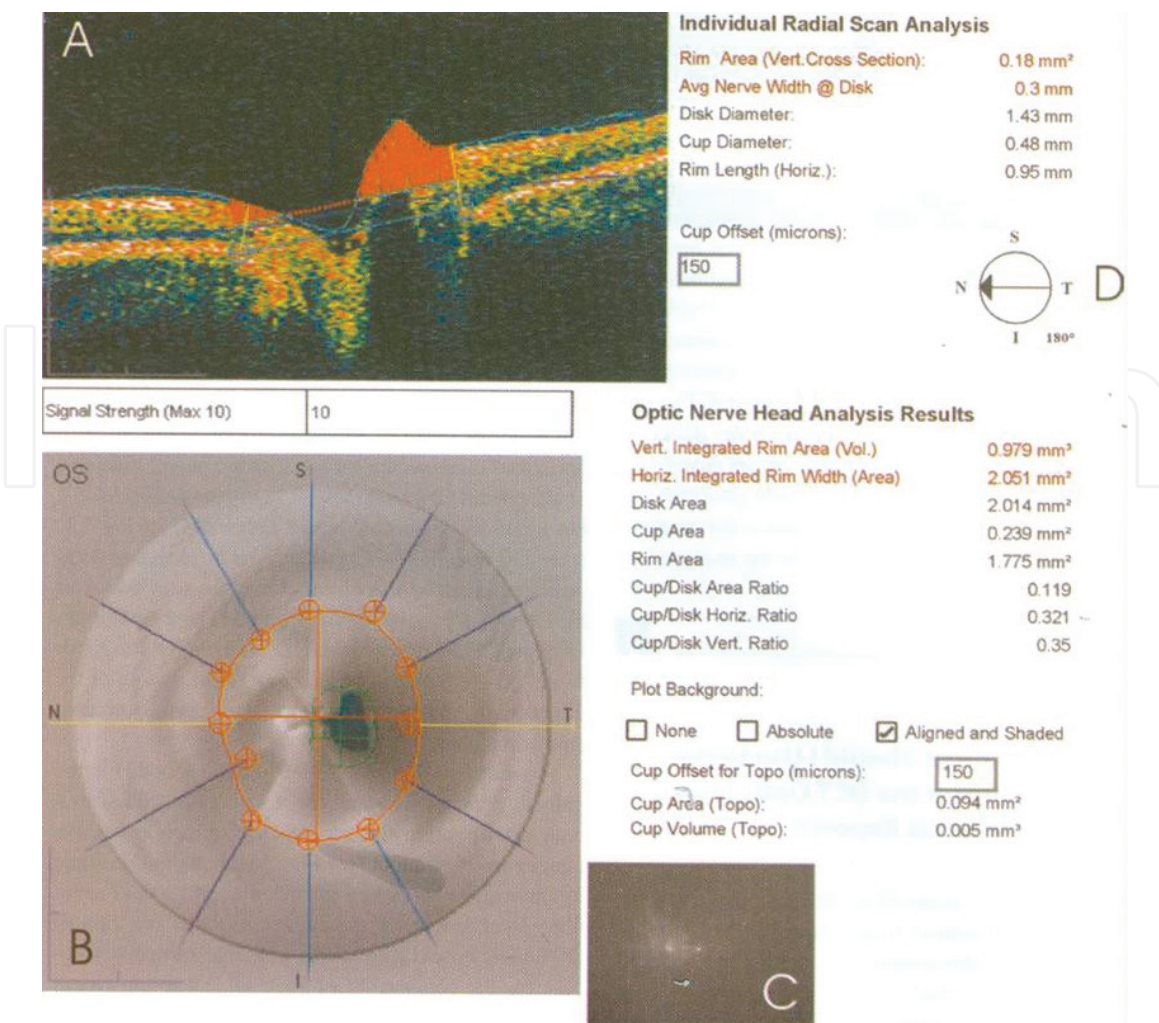


**Figure 3.** Optic nerve head analysis report (adapted from Carl Zeiss OCT Manual).

lines consists of 128 A scans crossing an area of 4 mm in length vertically with a total scan time of 1.92 s. The optic nerve head analysis report consists of a B scan image of the optic nerve head taken horizontally and an overall gray scale image of the optic disc demonstrating the disc and the cup margins (**Figure 3**).

The parameters for individual radial scan analysis are derived from an algorithm which takes into account the location of the inner limiting membrane (ILM) and the termination of the retinal pigment epithelium (RPE layer)/Bruch's membrane. Since the RPE/Bruch's termination defines the edge of the disc margin the horizontal distance between the two points on the RPE/Bruch's termination gives the disc diameter. A second line is drawn 150  $\mu\text{m}$  above and parallel to the one connecting the two points on the RPE/Bruch's termination. This is the plane that separates the rim from the cup. The cup diameter is the horizontal distance between the two points of intersection of this line with the ILM. Rim length is the difference between the cup diameter and the rim diameter. The rim area is total area above this line. The optic nerve head analysis is a conglomeration of all six radial scans arranged in a spoke pattern and interpolation of data between each of the scans created by smooth lines created around the disc and cup margins. Disc and cup areas are computed as the area within these margins, and rim area is calculated as the disc area minus cup area. The cup disc ratios (both horizontal and vertical) are calculated by the maximum distances of the disc and cup margins in the horizontal and vertical meridian, respectively. The vertical integrated rim area is an area interpolated around the discs of individual scans to define a rim volume. The horizontal integrated rim width is the mean of average nerve widths multiplied by the value

of circumference of the disc. The major limitation of the fast scan is the need for interpolation of data between the spaces which assumes that the six scans each time has been centered exactly at the same line. Hence, significant eye movements during a scan lead to loss of focal defects.

### 8.1.2 The retinal nerve fiber layer (RNFL) analysis

The RNFL analysis involves a fast RNFL scan which takes approximately 1.9 s and acquires three fast circular scans 3.4 mm around the disc. This is time-efficient scan alignment and placement is required only once, each scan having an automated segmentation algorithm that detects the ILM boundary, the RNFL, and the ganglion cell body layer.

RNFL map comprises of six circular scans of 1.44, 1.69, 2.25, 2.73, and 3.40 mm radii. The scan size is 2.27 times the radius of the ONH. It helps to measure RNFL thickness with accuracy in various disc sizes. Centration of the circle around the disc is shown as an image adjacent to the scans and decentration of this circle can lead to erroneous results for RNFL thickness as closer circle position to the disc gives a thicker RNFL measurement while a position far away gives thinner readings.

The RNFL thickness is reported as overall average thickness and averages by quadrants and clock hours. The average RNFL thickness and various comparisons within the same and the other eye is also projected in a tabular form (Figure 4).

RNFL thickness map typically has a double hump pattern as the RNFL is thicker at the superior and inferior poles. The thickness of RNFL of a patient is compared to age matched normative data base and interpreted in different color codings. The green color encompasses the 5th to 95th percentile of the normative range for RNFL and is considered normal. The yellow color represents first to fifth percentile of the normal population and considered borderline. Anything below the first percentile

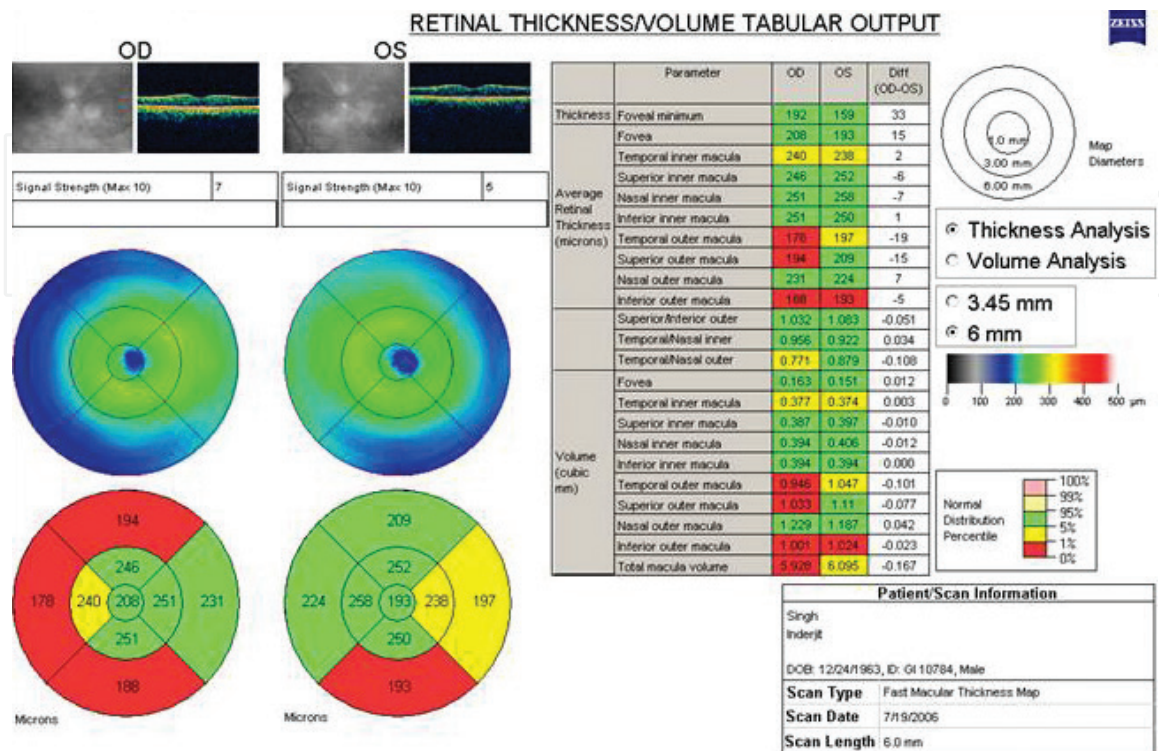
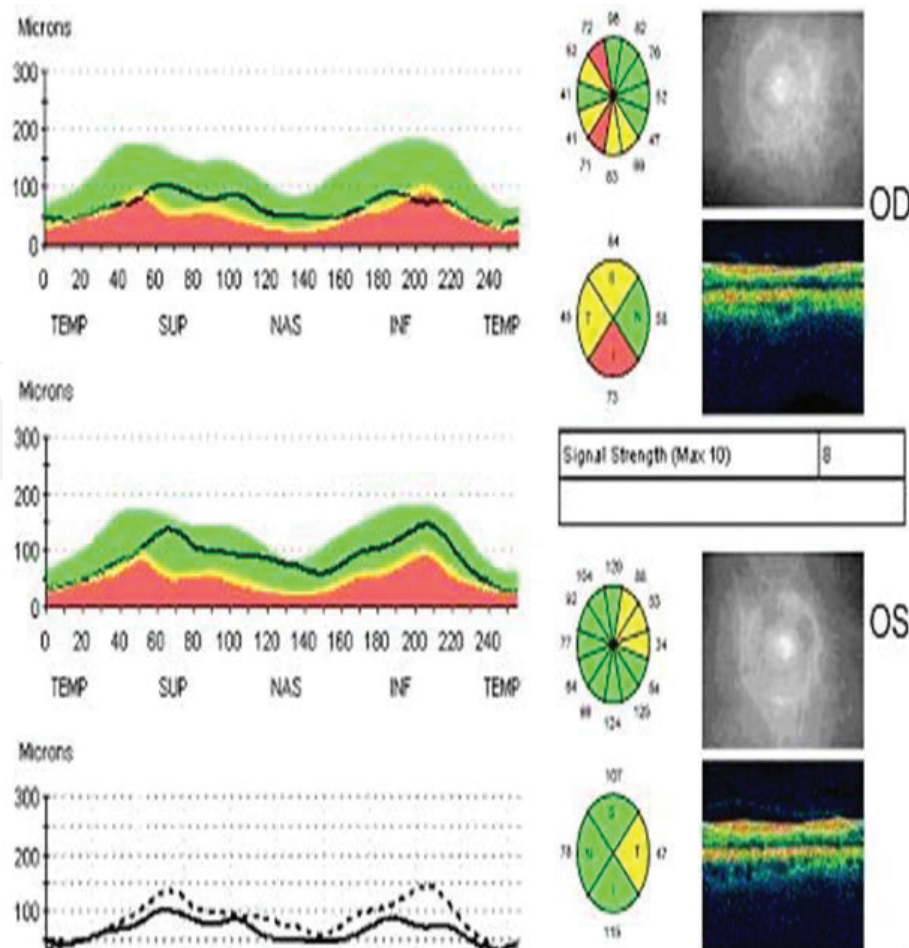


Figure 4. Retinal nerve fiber layer thickness/volume tabular output.



**Figure 5.**  
 RNFL thickness average analysis report (Stratus OCT: Carl Zeiss Meditec, Inc.).

is shown in red and considered outside normal limits. Values greater than 95th percentile are indicated in white and depicts above normal values (**Figure 5**).

## 8.2 Fourier domain OCT (FD-OCT) in glaucoma diagnosis

The newer generation Fourier-domain optical coherence tomography (FD-OCT) technology offers tremendous advances over the traditional time-domain (TD) technology in terms of speed and resolution. Currently, the Cirrus high-definition (HD)-OCT and RTVue 100 are commercially used to quantify peripapillary RNFL thickness in clinical practice. Studies indicate that RNFL thickness parameters measured on Cirrus OCT are reproducible and have high diagnostic sensitivity and specificity in discriminating between healthy and glaucomatous eyes [10, 11]. Furthermore, for the detection of glaucoma RNFL parameters of the RTVue-100 OCT have shown high specificity [12]. Studies indicate that ganglion cells located in the macular area are the earliest cells to be lost in glaucoma and hence this has led to utilize the less explored parameter of various OCT devices, the ganglion cell complex located in the macular region [13].

### 8.2.1 Optic nerve head scan pattern

The ONH scan is a combination of circular scans for RNFL thickness analysis and radial scans for ONH shape analysis. Combining circular scans and radial scans into one single pattern ensures that the RNFL scan and ONH scan naturally share same center. The scan time is only 0.5 s to help minimize any effect of eye movement. Hence the scan consists of 13 circles with diameters of 1.3–4.9 mm, which is used to



create circumpapillary nerve fiber (NFL) map and 12 radial lines with 3.7 mm length, which are used to calculate the disc margin which forms the ONH scan. All B-scans (lines) are centered at the optic disc.

### 8.2.2 Three dimensional disc scan pattern

The three dimensional (3D) disc scan provides high definition OCT image both at horizontal and vertical direction for ONH. The 3D disc scan covers a default 5 mm × 5 mm square region and is adjustable. It contains 101 horizontal lines. The 3D disc scan contains a total of 51,813 A-scans and takes 2.2 s. The analysis includes B-scan fly through, 3D display, and en face summation of intensity in a retinal sub-layer or band. The 3D scan also creates a high definition OCT SLO projection as a baseline for registration of the ONH scan between multiple visits. Yellow indicates a borderline result. Thickness measures with a p-value less than 1% are colored red to indicate an outside normal limits result.

### 8.2.3 Diagnostic parameters

The RNFL thickness profile is divided into 16 sectors and the sector averages are displayed outside of RNFL thickness map. Thickness measurement is compared with normative database with a probability value (p-value) between 5 and 95% shown as green color to indicate within normal limits. Thickness measures with a p-value less than 5% are colored yellow to indicate a borderline result and a p-value less than 1% are colored red to indicate thickness outside normal limits (**Figure 6**).

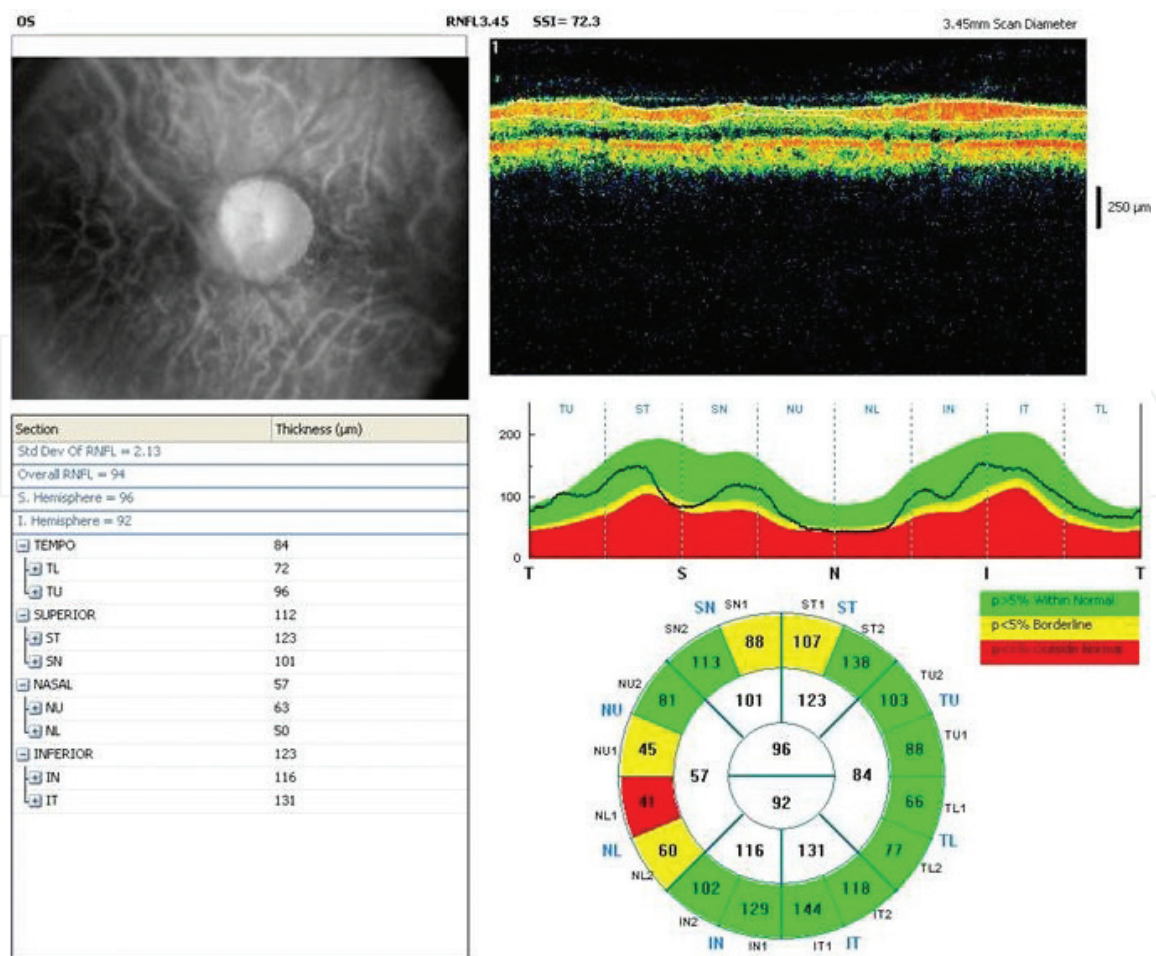


**Figure 6.** RNFL thickness average analysis (Optovue A4 Version).

### 8.2.4 Ganglion cell complex

The diagnosis of glaucoma was improved by concentrating on the ganglion cell complex rather than the entire retinal thickness. The ganglion cell complex is a three layered structure consisting of the nerve fiber, ganglion cell and inner plexiform layers (**Figure 7**).

It has been shown that glaucoma predominantly causes thinning of the GCC [14, 15]. The GCC scan consists of three-dimensional scans of the macular region that samples the macula with 14,928 A-scans over a 7-mm square area. The scan pattern consists of 1 horizontal line and 15 vertical lines at 0.5-mm intervals. The center of the GCC scan is shifted 0.75 mm temporally to improve sampling of the temporal periphery.

The GCC scan quantifies the thickness in all three retina layers affected by glaucoma thereby causing the ganglion cell layer to become thinner as glaucoma progresses. Since the macula contains 50% of all ganglion cells in the retina, GCC scan analysis is a robust method of assessing early ganglion cell loss in glaucoma.

#### 8.2.4.1 Ganglion cell map displays

Ganglion cell layer results are displayed in terms of three maps (**Figure 8**). The thickness map is color coded in a manner that brighter colors (red and orange) represent thicker areas and cooler colors (blue and green) represent thinner areas. Fovea has no ganglion cells and so is very thin (black spot).

In addition to the GCC thickness map, two other maps are also calculated and displayed on the analysis page for the GCC scan. A deviation map is calculated based on comparing the thickness map to the normative databases. The percent deviation is displayed with a color map where dark colors mean loss. Yellow and red are above average GCC (no loss). Blue is around 20% GCC loss and black is 50% loss or greater. The significance map is the GCC thickness map compared to the normal database at each single point, with probability values. Any point with thickness

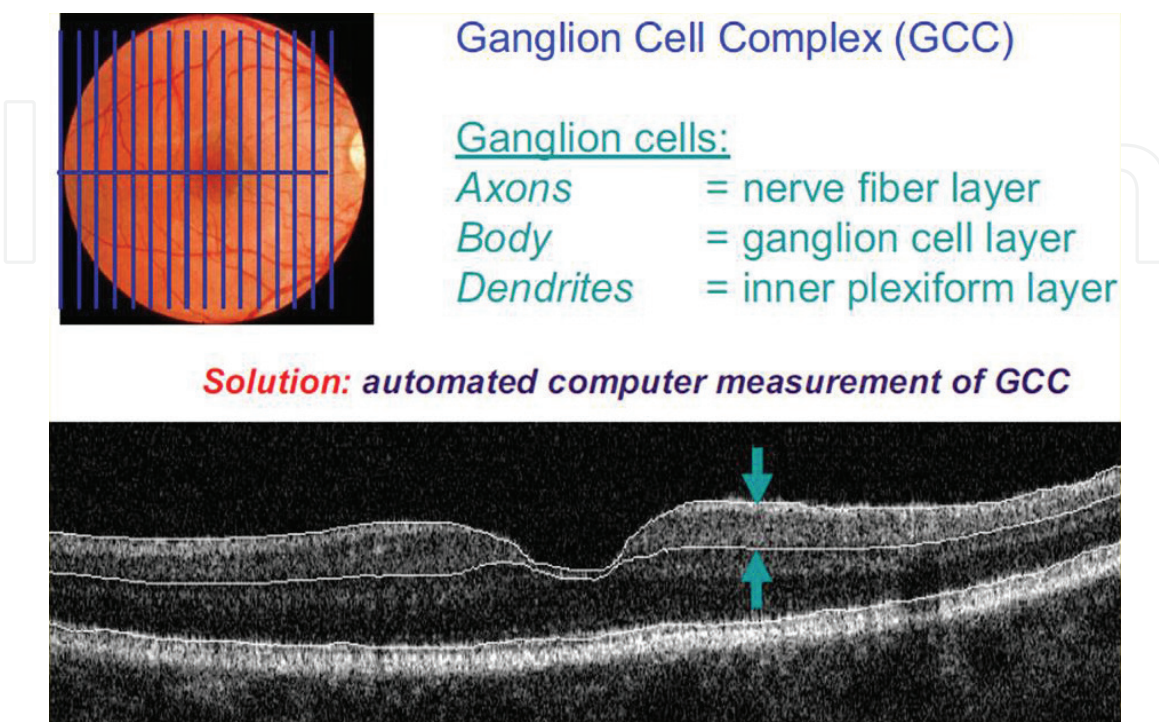


**Figure 7.**  
Ganglion cell complex.

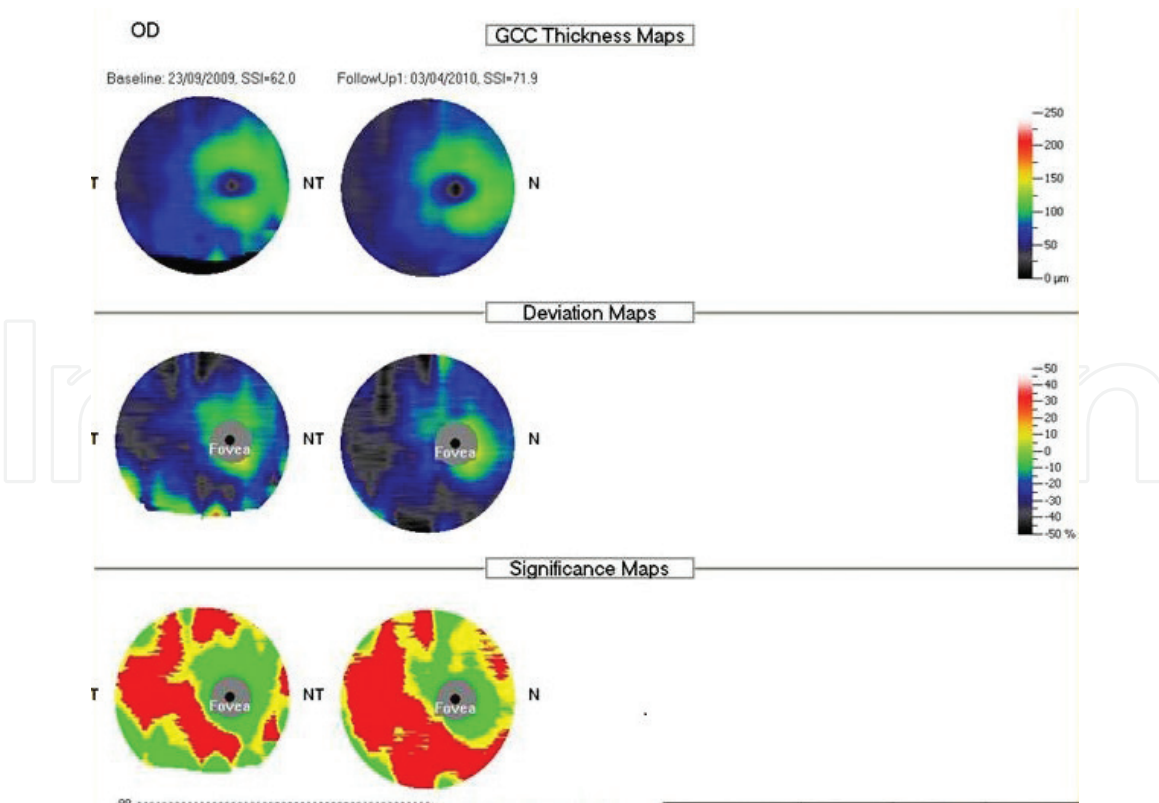


**Figure 8.**  
*GCC map displays (Optovue: RTVue Version A4).*

under 5% of the normal population is labeled as borderline with a yellow color and thickness under 1% is labeled as outside normal limits and has a red color. A green color means above the 5% of normal population.

## 9. Determining progression using OCT

Glaucoma is a progressive disorder and monitoring progression forms a quintessential part of glaucoma management. Quantitative assessment of progression can be done in a predictable manner using OCT as compared to the qualitative and subjective assessment of the optic nerve head using optic disc photographs. There exists an inherent variability of each machine which is calculated in each machine by repeated measurements preferably the same day. Any change amounting to two to three times the standard deviation of the machine is taken as a real change in terms of progression. In Stratus OCT, the measurement variability is markedly lower for RNFL scans as compared to ONH analysis thereby making RNFL scans a better method in determining changes over time or what is termed as true progression.

Glaucoma progression is either event based or trend based according to statistical analysis. In event analysis, a threshold is determined and true progression is said to have occurred when a follow-up measurement exceeds this preestablished threshold. Any change below this threshold is considered to be due to natural age-related loss or measurement variability. Event analysis thus, is intended to identify a gradual change over time crossing the threshold or development of a sudden event that falls above the predetermined threshold. On the contrary, a trend analysis identifies progression by monitoring the behavior of a parameter over time. This method is therefore, less sensitive to sudden change and the variability among consecutive tests.

## 9.1 Progression with time domain OCT

Progression with time domain OCT mostly utilizes the RNFL thickness measurements as these have shown to discriminate well between normal and glaucomatous eyes [16, 17]. Both diffuse and localized glaucomatous RNFL defects in the peripapillary area have shown to have good reproducibility with low intra-test and inter-test variability and can be utilized in determining progression [18–24]. Based on the published data on the repeatability of mean RNFL thickness measurements, any decrease in thickness exceeding 6.4–8  $\mu\text{m}$  can be considered to be abnormal and beyond the limits of test-retest variability with 95% tolerance [25]. These values are used only for mean peripapillary RNFL thickness and not for quadrants and clock hours as the variability is significantly higher in these areas owing to the shifts in scan locations.

The guided progression analysis (GPA) is a trend-based analysis that uses a linear regression to report change in overall mean RNFL thickness over time and also provides the significance of this change. The point of concern with the GPA analysis of Stratus OCT is that statistical significance reported doesn't take into consideration the rate of normal age-related loss. Therefore, some normal age-related changes may be reported as significant even though they do not represent true disease progression. The average age-related RNFL loss is expected to be between 0.16 and 0.31  $\mu\text{m}/\text{year}$  [26–28].

## 9.2 Progression with spectral domain OCT

The substantial increase in SD-OCT scanning speed over TD-OCT makes scans less prone to eye movement artifacts. Studies have reported excellent intra-visit and inter-visit measurement reproducibility for SD-OCT [29–34], superior to TD-OCT [35–37]. This makes the SD-OCT a potential tool in monitoring glaucoma progression.

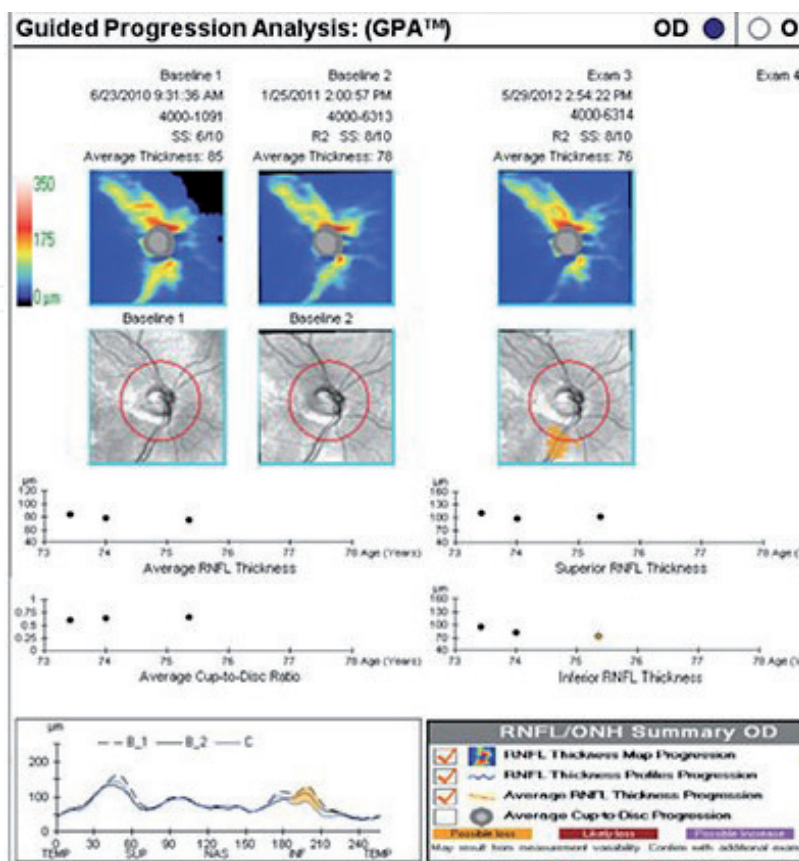
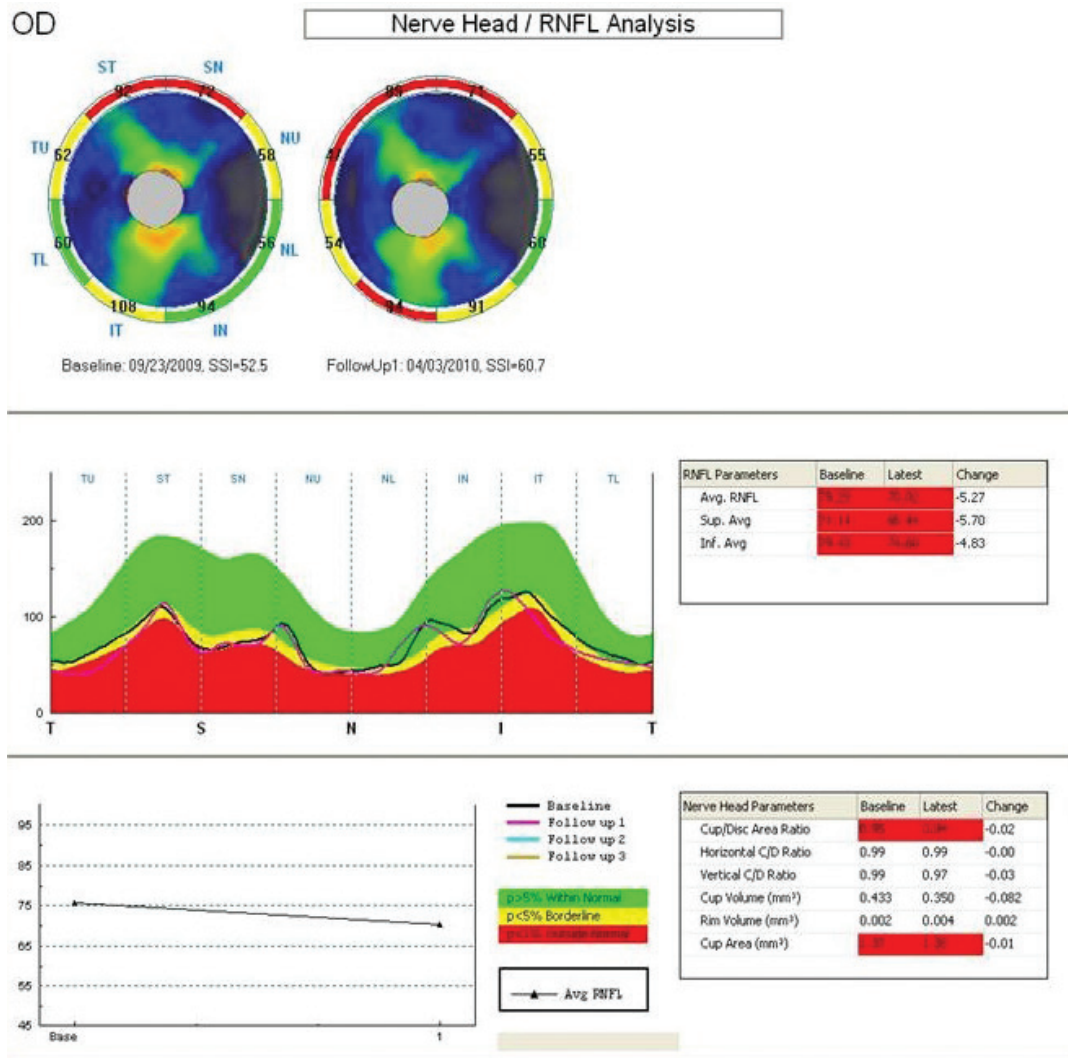


Figure 9. Cirrus SD-OCT RNFL-guided progression analysis (adapted Carl Zeiss Meditec, Dublin, CA).



**Figure 10.** RNFL change analysis (adapted: Optovue, Fremont, CA).

Ganglion cell complex diagnostic accuracy for detecting glaucoma has been shown to be similar to that of peripapillary RNFL thickness making it potentially valuable for monitoring glaucoma progression [38–42].

Progression analysis is currently available with Cirrus HD-OCT (Carl Zeiss Meditec, Dublin, CA) and RTVue (Optovue, Fremont, CA). Of these two devices, statistical analyses in form of event- and trend-based mechanism for progression detection is available only in the Cirrus HD-OCT. Data sampling of the RNFL is obtained from the 3.4-mm diameter peripapillary circle and the software also displays RNFL thickness changes from baseline for each pixel in the scanned area. Possible or likely RNFL thickness loss is reported if change exceeds the expected test-retest variability in a single or two consecutive follow-up examinations, respectively. In addition, linear regression is performed to determine the rate of change, confidence limits, and statistical significance of the trend (Figure 9).

The RTVue offers progression analysis that includes side-by-side RNFL thickness measurements and overlay of the RNFL profiles for the consecutive scans. The RTVue also provides similar analysis for ganglion cell complex thickness along with thickness change plots (Figure 10). However, a formal statistical analysis of change over time is not currently included in the latest version of the software for this device (version 6.1) (Figure 11).

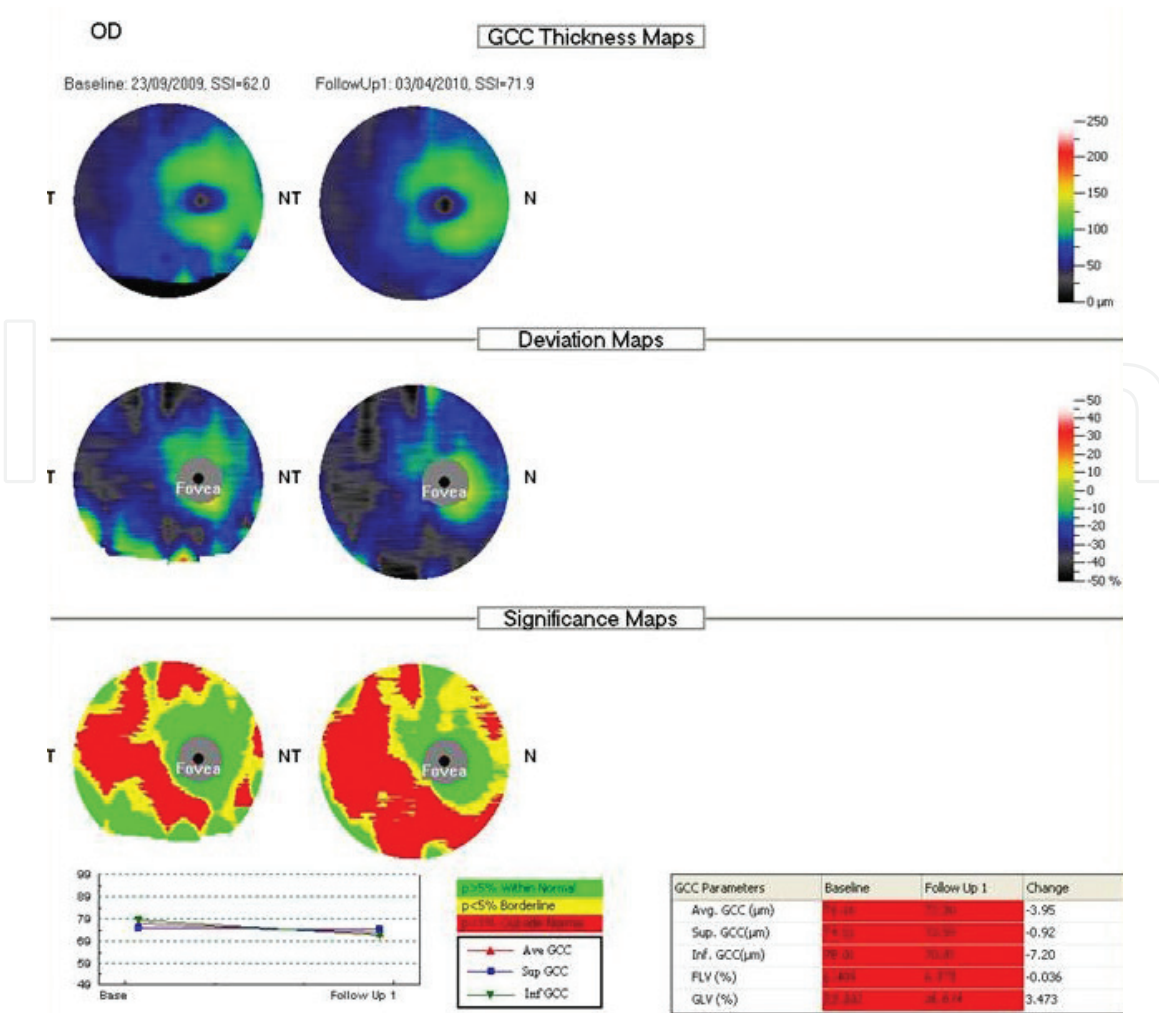


**Figure 11.** Ganglion cell analysis showing progression (adapted: Optovue, Fremont, CA).

## 10. Anterior segment OCT (AS-OCT)

Anterior segment OCT (AS-OCT) imaging initially described by Izatt et al. using the same wavelength of light as retinal OCT [43]. However, the 830 nm wavelength was found to be suboptimal for imaging the angle due to limited penetration through scattering tissue such as the sclera. Hence, a newer OCT imaging of the anterior segment with a longer wavelength of 1310 nm was developed that had the advantages of better penetration through sclera [44]. Currently, there are two dedicated anterior segment devices commercially available. The SL-OCT (Heidelberg Engineering) and the Visante (Carl Zeiss Meditec, Inc.) Newer Fourier domain anterior segment OCT devices however have been developed, and these allow rapid three-dimensional cube scanning of the anterior segment.

### 10.1 Qualitative assessment using AS-OCT

An important landmark to identify when interpreting AS-OCT images is the scleral spur. This is visible as an inward projection of the sclera at the junction between the inner scleral and corneal curvatures. Studies have shown that scleral spur may not be visible in 25% cases [45]. The apposition between the iris and the inner corneo-scleral wall has been used in several studies as a qualitative method

of detecting closure of the anterior chamber angle [46, 47]. The degree of apposition however may not correlate exactly with appositional closure as defined by gonioscopy.

## 10.2 Quantitative assessment using AS-OCT

An in-built software in most of the AS-OCT helps in quantitative measurement of the anterior chamber angle. Several parameters designated for the quantitative analysis has shown good reproducibility [48–50]. Difficulty in visualizing the scleral spur and the wide natural variation in angle anatomy within the same eye as well as between eyes are limiting factors in the routine use of quantitative measurement for angle assessment.

The various quantitative parameters reported are as follows (**Figure 12a–c**):

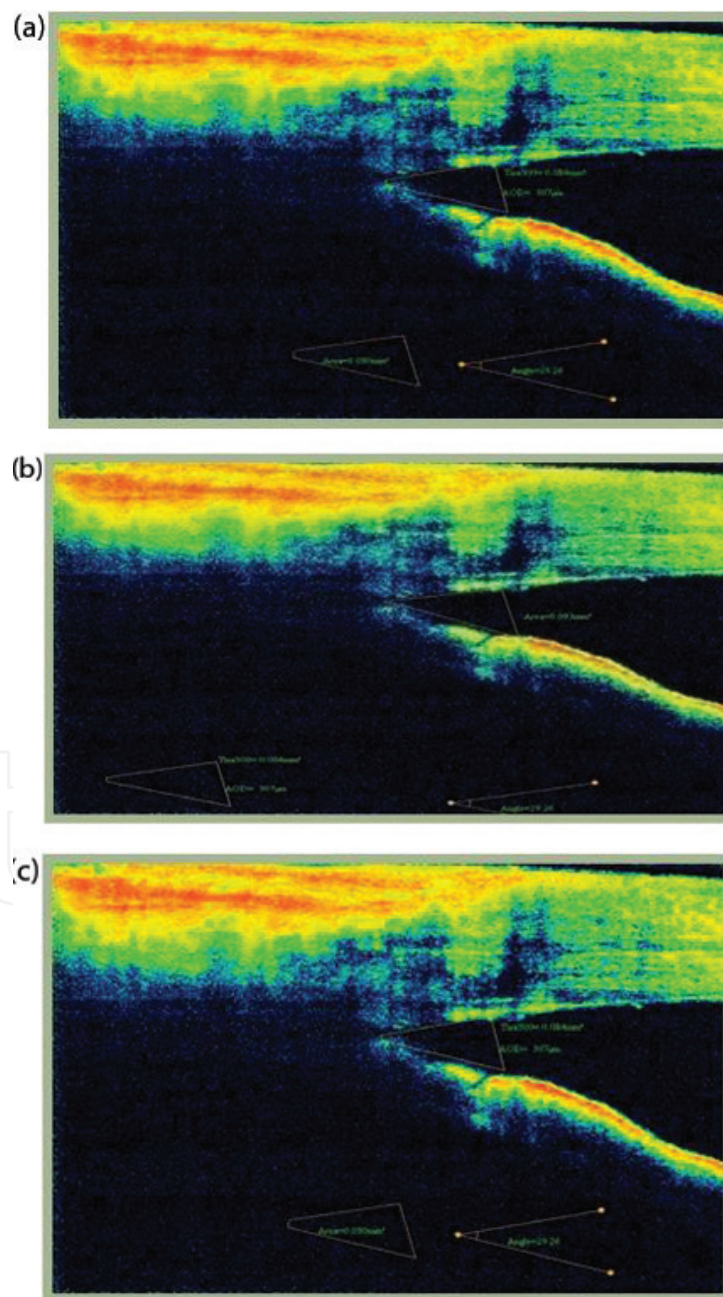


**Figure 12.** Quantitative measurement of (a) angle opening distance using RTVue anterior segment OCT, (b) angle recess area using RTVue anterior segment OCT, and (c) trabeculo-iris space area using RTVue anterior segment OCT.

- a. Angle opening distance (AOD in mm): it is the perpendicular distance between a point 500  $\mu\text{m}$  (AOD 500) or 750  $\mu\text{m}$  (AOD750) anterior to the scleral spur and the opposing iris.
- b. Angle recess area (ARA in  $\text{mm}^2$ ): it is a triangular area (ARA 500 or 750) bounded by the AOD 500 or 750, the anterior iris surface, and the inner corneo-scleral wall.

Trabecular space area (TISA in  $\text{mm}^2$ ): it is the trapezoidal area (TISA 500 or 750) bounded by the AOD 500 or 750, the anterior iris surface, the inner corneo-scleral wall, and the perpendicular distance between the scleral spur and the opposing iris.

### **10.3 Clinical applications**

In clinical glaucoma practice, AS-OCT is used as an adjunct to gonioscopy. It can act as a substitute when gonioscopy is not feasible due to corneal pathology or lack of patient co-operation. Furthermore, it is extremely useful as a patient education tool, to explain the pathophysiology of angle closure to patients before any laser procedures like peripheral iridotomy. Its advantages over gonioscopy lie in the fact that it is a non-contact procedure and can be performed under dark conditions allowing angle assessment during physiological mydriasis. A major limitation however is its inability to visualize the structures behind the iris. This limits its ability in diagnosing the posterior mechanisms of angle closure such as iridociliary lesions and plateau iris. AS-OCT may also be used to visualize trabeculectomy blebs and anterior segment implants such as drainage devices and keratoprosthesis—however, the clinical value in these situations appears to be limited.

## **11. Conclusion**

Advances in OCT technology have made it possible to apply OCT in a wide variety of applications. The high depth and transversal resolution in OCT and the ability to decouple depth resolution from transverse resolution make it an important tool in ophthalmic imaging. Few other advantages are high probing depth in scattering media, contact free, and non-invasive operation, and the possibility to create various function-dependent image contrasting methods.

### **11.1 Limitations**

1. Because OCT utilizes light waves (unlike ultrasound which uses sound waves), media opacities such as vitreous hemorrhage, dense cataract, or corneal opacities can interfere with optimal imaging.
2. Motion artifacts: eye movements can sometimes diminish the quality of the image. However with the spectral domain shortened acquisition, time often results in fewer motion related artifacts.
3. Learning curve: acquiring good quality images are an art and has a learning curve. Although with the advent of newer technologies, such as spectral domain acquisition or the use of eye tracking equipment, the likelihood of such acquisition error has been reduced dramatically.



IntechOpen

### **Author details**

Baswati Sahoo<sup>1\*</sup> and Julie Pegu<sup>2</sup>

1 Ahalia Hospital, Abu Dhabi, United Arab Emirates

2 Dr. Shroffs Charity Eye hospital, New Delhi, India

\*Address all correspondence to: bpsceh@gmail.com

### **IntechOpen**

---

© 2019 The Author(s). Licensee IntechOpen. This chapter is distributed under the terms of the Creative Commons Attribution License (<http://creativecommons.org/licenses/by/3.0>), which permits unrestricted use, distribution, and reproduction in any medium, provided the original work is properly cited. 

## References

- [1] Bathija R, Gupta N, Zangwill L, et al. Changing definition of glaucoma. *Journal of Glaucoma*. 1998;7(3):165-169
- [2] Gordon MO, Torri V, Miglior S. Validated prediction model for the development of primary open-angle glaucoma in individuals with ocular hypertension. *Ophthalmology*. 2007;114:10-19
- [3] Sommer A, Katz J, Quigley HA, Miller NR, Robin AL, Richter RC. Clinically detectable nerve fiber atrophy precedes the onset of glaucomatous field loss. *Archives of Ophthalmology*. 1991;109:77-83
- [4] Medeiros FA, Zangwill LM, Bowd C, Sample PA, Weinreb RN. Use of progressive glaucomatous optic disk change as the reference standard for evaluation of diagnostic tests in glaucoma. *American Journal of Ophthalmology*. 2005;139:1010-1018
- [5] Caprioli J, Nouri-Mahdavi K, Law SK, Badalà F. Optic disc imaging in perimetrically normal eyes of glaucoma patients with unilateral field loss. *Transactions of the American Ophthalmological Society*. 2006;104:202-211
- [6] Airaksinen PJ, Tuulonen A, Werner EB. Clinical evaluation of the optic disc and retinal nerve fiber layer. In: Ritch R, Shields MB, Krupin T, editors. *The Glaucomas*. St. Louis: Mosby; 1996. pp. 617-657
- [7] Sull AC, Vuong LN, Price LL, et al. Comparison of spectral/Fourier domain optical coherence tomography instruments for assessment of normal macular thickness. *Retina*. 2010;30:235-245
- [8] de Boer JF, Cense B, Park BH, et al. Improved signal-to-noise ratio in spectral-domain compared with time-domain optical coherence tomography. *Optics Letters*. 2003;28:2067-2069
- [9] Leitgeb R, Hitzenberger C, Fercher A. Performance of Fourier domain vs. time domain optical coherence tomography. *Optics Express*. 2003;11:889-894
- [10] Mwanza JC, Oakley JD, Budenz DL, Anderson DR. Cirrus Optical Coherence Tomography Normative Database Study Group. Ability of cirrus HD-OCT optic nerve head parameters to discriminate normal from glaucomatous eyes. *Ophthalmology*. 2011;118:241-280
- [11] Sung KR, Na JH, Lee Y. Glaucoma diagnostic capabilities of optic nerve head parameters as determined by cirrus HD optical coherence tomography. *Journal of Glaucoma*. 2012;21:498-504
- [12] Paul C. To assess the glaucoma diagnostic ability of Fourier domain optical coherence tomography. *American Journal of Engineering Research*. 2013;10:155-169
- [13] Hood DC, Raza AS, de Moraes CG, Liebmann JM, Ritch R. Glaucomatous damage of the macula. *Progress in Retinal and Eye Research*. 2013;32:1-21
- [14] Medeiros FA, Zangwill LM, Bowd C, Vessani RM, Susanna R Jr, Weinreb RN. Evaluation of retinal nerve fiber layer, optic nerve head, and macular thickness measurements for glaucoma detection using optical coherence tomography. *American Journal of Ophthalmology*. 2005;139:44-55
- [15] Budenz DL, Michael A, Chang RT, McSoley J, Katz J. Sensitivity and specificity of the StratusOCT for perimetric glaucoma. *Ophthalmology*. 2005;112:3-9

- [16] Medeiros FA, Zangwill LM, Bowd C, Weinreb RN. Comparison of the GDx VCC scanning laser polarimeter, HRT II confocal scanning laser ophthalmoscope, and stratus OCT optical coherence tomograph for the detection of glaucoma. *Archives of Ophthalmology*. 2004;**122**:827-837
- [17] Wollstein G, Ishikawa H, Wang J, Beaton SA, Schuman JS. Comparison of three optical coherence tomography scanning areas for detection of glaucomatous damage. *American Journal of Ophthalmology*. 2005;**139**:39-43
- [18] Bowd C, Zangwill LM, Berry CC, et al. Detecting early glaucoma by assessment of retinal nerve fiber layer thickness and visual function. *Investigative Ophthalmology & Visual Science*. 2001;**42**:1993-2003
- [19] Blumenthal EZ, Williams JM, Weinreb RN, Girkin CA, Berry CC, Zangwill LM. Reproducibility of nerve fiber layer thickness measurements by use of optical coherence tomography. *Ophthalmology*. 2000;**107**:2278-2282
- [20] Budenz DL, Chang RT, Huang X, Knighton RW, Tielsch JM. Reproducibility of retinal nerve fiber thickness measurements using the stratus OCT in normal and glaucomatous eyes. *Investigative Ophthalmology & Visual Science*. 2005;**46**:2440-2443
- [21] Budenz DL, Fredette MJ, Feuer WJ, Anderson DR. Reproducibility of peripapillary retinal nerve fiber thickness measurements with stratus OCT in glaucomatous eyes. *Ophthalmology*. 2008;**115**:661-666
- [22] Paunescu LA, Schuman JS, Price LL, et al. Reproducibility of nerve fiber thickness, macular thickness, and optic nerve head measurements using Stratus OCT. *Investigative Ophthalmology & Visual Science*. 2004;**45**:1716-1724
- [23] Schuman JS, Pedut-Kloizman T, Hertzmark E, et al. Reproducibility of nerve fiber layer thickness measurements using optical coherence tomography. *Ophthalmology*. 1996;**103**:1889-1898
- [24] Gurses-Ozden R, Teng C, Vessani R, Zafar S, Liebmann JM, Ritch R. Macular and retinal nerve fiber layer thickness measurement reproducibility using optical coherence tomography (OCT-3). *Journal of Glaucoma*. 2004;**13**:238-244
- [25] Lee EJ, Kim TW, Park KH, Seong M, Kim H, Kim DM. Ability of stratus OCT to detect progressive retinal nerve fiber layer atrophy in glaucoma. *Investigative Ophthalmology & Visual Science*. 2009;**50**:662-668
- [26] Budenz DL, Anderson DR, Varma R, et al. Determinants of normal retinal nerve fiber layer thickness measured by stratus OCT. *Ophthalmology*. 2007;**114**:1046-1052
- [27] Parikh RS, Parikh SR, Sekhar GC, Prabakaran S, Babu JG, Thomas R. Normal age-related decay of retinal nerve fiber layer thickness. *Ophthalmology*. 2007;**114**:921-926
- [28] Harwerth RS, Wheat JL, Rangaswamy NV. Age-related losses of retinal ganglion cells and axons. *Investigative Ophthalmology & Visual Science*. 2008;**49**:4437-4443
- [29] Garas A, Vargha P, Hollo G. Reproducibility of retinal nerve fiber layer and macular thickness measurement with the RTVue-100 optical coherence tomograph. *Ophthalmology*. 2010;**117**:738-746
- [30] Gonzalez-Garcia AO, Vizzeri G, Bowd C, Medeiros FA, Zangwill LM, Weinreb RN. Reproducibility of RTVue retinal nerve fiber layer

thickness and optic disc measurements and agreement with stratus optical coherence tomography measurements. *American Journal of Ophthalmology*. 2009;**147**:1067-1074

[31] Lee SH, Kim SH, Kim TW, Park KH, Kim DM. Reproducibility of retinal nerve fiber thickness measurements using the test-retest function of spectral OCT/SLO in normal and glaucomatous eyes. *Journal of Glaucoma*. 2010;**19**:637-642

[32] Li JP, Wang XZ, Fu J, Li SN, Wang NL. Reproducibility of RTVue retinal nerve fiber layer thickness and optic nerve head measurements in normal and glaucoma eyes. *Chinese Medical Journal*. 2010;**123**:1898-1903

[33] Mwanza JC, Chang RT, Budenz DL, et al. Reproducibility of peripapillary retinal nerve fiber layer thickness and optic nerve head parameters measured with Cirrus™ HD-OCT in glaucomatous eyes. *Investigative Ophthalmology & Visual Science*. 2010;**51**:5724-5730

[34] Menke MN, Knecht P, Sturm V, Dabov S, Funk J. Reproducibility of nerve fiber layer thickness measurements using 3D fourier-domain OCT. *Investigative Ophthalmology & Visual Science*. 2008;**49**:5386-5391

[35] Schuman JS. Spectral domain optical coherence tomography for glaucoma (an AOS thesis). *Transactions of the American Ophthalmological Society*. 2008;**106**:426-458

[36] Leung CK, Cheung CY, Weinreb RN, et al. Retinal nerve fiber layer imaging with spectral-domain optical coherence tomography: A variability and diagnostic performance study. *Ophthalmology*. 2009;**116**:1257-1263

[37] Kim JS, Ishikawa H, Sung KR, et al. Retinal nerve fibre layer thickness measurement reproducibility improved

with spectral domain optical coherence tomography. *The British Journal of Ophthalmology*. 2009;**93**:1057-1063

[38] Garas A, Vargha P, Hollo G. Diagnostic accuracy of nerve fibre layer, macular thickness and optic disc measurements made with the RTVue-100 optical coherence tomograph to detect glaucoma. *Eye*. 2011;**25**:57-65

[39] Kim NR, Lee ES, Seong GJ, et al. Comparing the ganglion cell complex and retinal nerve fibre layer measurements by Fourier domain OCT to detect glaucoma in high myopia. *The British Journal of Ophthalmology*. [published online ahead of print October 17, 2010]

[40] Rao HL, Zangwill LM, Weinreb RN, Sample PA, Alencar LM, Medeiros FA. Comparison of different spectral domain optical coherence tomography scanning areas for glaucoma diagnosis. *Ophthalmology*. 2010;**117**:1692-1699

[41] Tan O, Chopra V, Lu AT, et al. Detection of macular ganglion cell loss in glaucoma by Fourier-domain optical coherence tomography. *Ophthalmology*. 2009;**116**:2305-2314

[42] Tan O, Li G, Lu AT, Varma R, Huang D. Mapping of macular substructures with optical coherence tomography for glaucoma diagnosis. *Ophthalmology*. 2008;**115**:949-956

[43] Izatt JA, Hee MR, Swanson EA, et al. Micrometer-scale resolution imaging of the anterior eye in vivo with optical coherence tomography. *Archives of Ophthalmology*. 1994;**112**:1584-1589

[44] Radhakrishnan S, Rollins AM, Roth JE, et al. Real-time optical coherence tomography of the anterior segment at 1310 nm. *Archives of Ophthalmology*. 2001;**119**:1179-1185

[45] Sakata LM, Lavanya R, Friedman DS, et al. Assessment of the scleral spur

in anterior segment optical coherence tomography images. *Archives of Ophthalmology*. 2008;**126**:181-185

[46] Nolan WP, See JL, Chew PT, et al. Detection of primary angle closure using anterior segment OCT in Asian eyes. *Ophthalmology*. 2007;**114**:33-39

[47] Lavanya R, Foster PJ, Sakata LM, et al. Screening for narrow angles in the Singapore population: Evaluation of new non-contact screening methods. *Ophthalmology*. 2008;**115**:1720-1727

[48] Radhakrishnan S, Goldsmith J, Westphal V, et al. Comparison of coherence tomography and ultrasound biomicroscopy for detection of narrow anterior chamber angles. *Archives of Ophthalmology*. 2005;**128**:1053-1059

[49] Fukuda S, Kawana K, Yasuno Y, et al. Repeatability and reproducibility of anterior ocular biometric measurements with 2-D and 3-D optical coherence tomography. *Journal of Cataract and Refractive Surgery*. 2010;**36**:1867-1873

[50] Tan AN, Sauren LD, de Brabander J, et al. Reproducibility of anterior chamber angle measurements with anterior segment OCT. *Investigative Ophthalmology & Visual Science*. 2011;**52**:2095-2099